Available online at www.sciencedirect.com
ScienceDirect
Optics Communications 281 (2008) 225–231
OPTICS COMMUNICATIONS
www.elsevier.com/locate/optcom

4-Port polarization-independent wavelength-interleaving bidirectional circulator

Po-Jen Hsieh [a,*], Jing-Heng Chen [b], Hung-Chih Hsieh [a], Zhi-Cheng Jian [a], Der-Chin Su [a]

[a] Department of Photonics & Institute of Electro-Optical Engineering, National Chiao-Tung University, 1001 Ta-Hsueh Road, Hsin-Chu 30050, Taiwan, ROC

[b] Department of Photonics, Feng-Chia University, 100 Wenhwa Road, Seatwen, Taichung 40724, Taiwan, ROC

Received 7 February 2007; received in revised form 22 August 2007; accepted 10 September 2007

Abstract

This study develops an alternative type of 4-port polarization-independent wavelength-interleaving bidirectional circulator. In this circulator the even- and odd-channels circulate with opposite handedness regardless of the state of polarization of signals. It has a pair of orthogonal holographic spatial- and polarization modules (HSPMs) and a Lyot-Ohman filter (LOF). Each HSPM has two holographic spatial walk-off polarizers (HSWPs), two glass plates and two half-wave plates. The function of the HSWP is firstly described. Next, the structures and the operating principles of the HSPM and the LOF are also described. Then, the operating principle and the performance of this circulator are discussed. It has such merits as polarization-independence, compactness, high isolation, lack of polarization mode dispersion and ease of fabrication.

Keywords: Optical communications; Holographic optical elements; Polarization

1. Introduction

Optical circulators [1,2] are important nonreciprocal devices that direct light from one port to another in one direction. Circulators are necessary components in the construction of foundational network modules, such as add/drop multiplexers [3], dispersion compensation [4], optical amplifiers [5] and time-domain reflectometry [6]. As the design of optical communication system becomes more complex, a bidirectional transmission device is becoming highly desirable because of its evident advantages over the unidirection transmission. However, bidirectional transmission in an optical communication system suffers from backreflection. To overcome this drawback, Tai et al. proposed a wavelength-interleaving bidirectional circulator [7], which consists of a polarization beam splitter (PBS), a Faraday rotating garnet, a Lyot-Ohman filter (LOF), a polarizer and a prism. Because of the function of the PBS, either the s- or the p-polarization component is operated in every route, and the other one is discarded. The valid polarization depends on the passage that is associated with route. Our previous paper proposed a holographic spatial walk-off polarizer (HSWP) [8] to replace the crystal-type spatial walk-off polarizer (SWP), and applied the HSWP to design a 4-port polarization-independent optical circulator with good performance. Based on a similar consideration, a holographic spatial- and polarization module (HSPM) is designed to replace a polarization beam splitter and a Faraday rotating garnet using two HSWPs, two glass plates and two half-wave plates. This study develops an alternative 4-port polarization-independent wavelength-interleaving bidirectional circulator. This circulator comprises an LOF and a pair of orthogonal HSPMs. To show its validity, the HSWPs for the 1550 nm wavelength were fabricated, and the diffraction efficiencies of the s- and p-polarizations measured. The characteristic parameters of the LOF were also measured.

* Corresponding author.
E-mail address: t7503@faculty.nctu.edu.tw (P.-J. Hsieh).

0030-4018/$ - see front matter © 2007 Elsevier B.V. All rights reserved.
doi:10.1016/j.optcom.2007.09.023

The operating principle and the performance of this circulator are discussed. This bidirectional optical circulator can be operated polarization-independently and with interleaving wavelengths.

2. Principles

2.1. Holographic spatial walk-off polarizer (HSWP) [8]

The HSWP is essentially a transmission-type phase volume holographic grating that is fabricated on a substrate. Fig. 1 depicts its structure and operating principle. The traveling of the light beam from left to right is shown in black and the reverse propagation is shown in gray; the symbols - - -, ⋯ and — represent unpolarized light, s-polarized light and p-polarized light, respectively. When unpolarized light is normally incident at point *A*, the s-polarized component is transmitted straight through the HSWP while the p-polarized component is completely diffracted toward point *B* and totally reflected at point *B*. The p-polarized component hits the grating again at point *C* and is totally reflected again. The reflected light from point *C* satisfies the Bragg condition of the grating, and the p-polarized component is then diffracted and parallel to the input light at point *A*, as shown in the left-upper circle. Consequently, two orthogonally polarized parallel beams with a separation of *d* can be obtained. However, if two separate s- and p-polarized light beams are normally incident on the HSWP at points *D* and *E*, then they will travel along the original paths in opposite directions. They are then merged into a single beam at *A*, which propagates out perpendicularly to the HSWP.

2.2. Holographic spatial- and polarization module (HSPM)

This study designs a new type of HSPM [8], which is composed of a pair of orthogonal HSWPs, two 45° half-wave plates (Hs) and two transparent glass plates (*G*s), as shown in Fig. 2a. The HSWP and the orthogonal HSWP separate the corresponding s- and p- polarizations of the incident beam along the *y*- and *x*-axes by the same distance, *d*. They are represented as $HSWP_y$ and $HSWP_x$ for convenience, respectively. *H*s and *G*s are located in the same plane; *H*s are in the first and the third quadrants, and *G*s are in the second and the fourth quadrants. To prevent the polarization mode dispersion (PMD), *H* and *G* must have the same optical thickness. The subscripts *u* and *l* refer upper and lower parts, respectively.

If two unpolarized light beams, shown in black and gray with separation *d* in the *x*-direction, are incident on the $HSWP_y$ as shown in Fig. 2a, then their *x*-polarization components will pass through $HSWP_y$ directly and their *y*-polarization components will be diffracted and propagate in parallel with the *x*-polarization components. Therefore, four beams are obtained. The separation between the upper beam and the lower beam is *d*; that between the left beam and the right beam is also *d*. Next, two of the beams pass through *H*s and their polarization planes are rotated by 90°. The other two pass through *G*s and their polarization planes remain unchanged. Finally, all of the beams are incident on the $HSWP_x$, and merge into two beams again. Each beam has two orthogonal polarization components originating from two corresponding incident beams. For clarity, the states of polarization (SOPs) and relative positions of the light beams after propagating each component are shown in the lower part of Fig. 2a. Here, a quadrantal diagram is used to show the positions of the beams, and the symbols, and represent unpolarization, *y*-polarization and *x*-polarization, respectively. The separation between the two symbols located in the neighboring quadrants is also *d*. Hence, the HSPM can change two unpolarized beams with separation *d* in the *x*-direction into two unpolarized beams with the same separation *d* in the *y*-direction. The polarization components of the two output beams originate from two corresponding incident beams.

If the HSPM is rotated by 180° about the *x*-axis, then its optical configuration is changed, as shown in Fig. 2b. For clarity, the module and each element are primed. Similarly, HSPM' can change two unpolarized beams separated by *d* in the *y*-direction into two unpolarized beams with the same separation *d* in the *x*-direction, and the polarization components of the two output beams also originate from two corresponding incident beams. The performance is similar to that of HSPM, as shown in Fig. 2b.

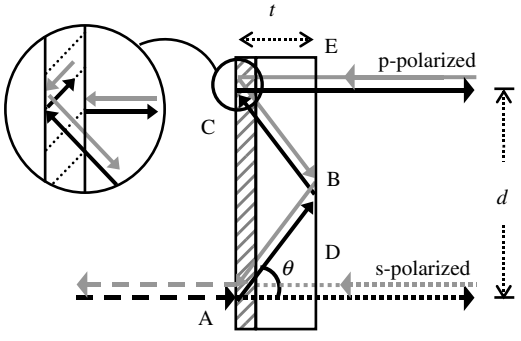

Fig. 1. Structure and operating principles of the holographic spatial walk-off polarizer.

2.3. Lyot-Ohman filter (LOF)

The same type of Lyot-Ohman filter [9] used by Cao et al. [10] is employed herein. It consists of three 45° half-wave plates (*H*s) and three identical groups of crystals. Each group of crystals consists of an YVO_4 and a TiO_2, whose thicknesses are L_y and L_t, respectively. One group of crystals is located between H_1 and H_2; the other two groups of crystals face in opposite directions and are located between H_2 and H_3, as shown in Fig. 3. If Δn_y and Δn_t are the differences of between the ordinary and extraordinary refractive indices, of the YVO_4 and the TiO_2, respectively, then the free spectral range (FSR) [9] of the LOF is given as

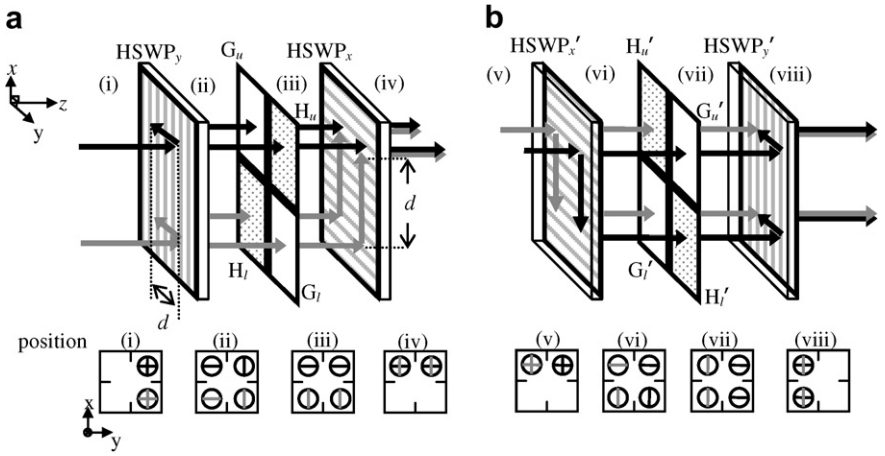

Fig. 2. Structure and operating principles of the proposed (a) HSPM and (b) HSPM′, and the associated SOPs.

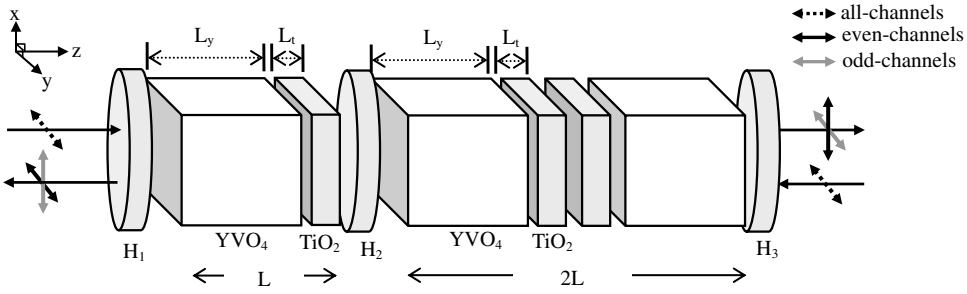

Fig. 3. Structure and operating principles of the Lyot-Ohman filter.

$$\mathrm{FSR} = \frac{c}{\Delta n_y L_y + \Delta n_t L_t}, \tag{1}$$

where c is the speed of light. Consequently, when an x-polarized or y-polarized light beam with central frequency f_c passes through the LOF in the $+z$ direction, the SOP is rotated by 90° if the frequency equals $f_c \pm (2m+1)\cdot \mathrm{FSR}$ (odd-channels), where m is an integer; and the SOP remains unchanged if the frequency equals $f_c \pm 2m \cdot \mathrm{FSR}$ (even-channels). If the light beam passes through the LOF in the $-z$ direction, then the SOPs of odd-channels remain unchanged and the SOPs of even-channels are rotated by 90°. To avoid confusion, Fig. 3 displays only the y-polarization of the incident beam, where the symbols ◂⋯▸, ↔, ⟷ and represent all-channels, even-channels and odd-channels, respectively. The x-polarization of the incident beam also has the same operations. Hence, the LOF can rotate the SOPs of the light beam by 90° with interleaving of wavelengths.

2.4. Bidirectional circulator

Based on the above principles, a module is designed by connecting an HSPM, an LOF and an HSPM' together in sequence. Fig. 4 depicts the operating principles; the input signal is plotted as dotted-lines, and the even- and odd-output channels are plotted as black lines and gray lines, respectively. If an input beam is normally incident on an HSPM from Port-1 at (0, 0), as shown in Fig. 4a, then two y-polarized beams with separation d in the y-direction are obtained. These two beams pass through the LOF; the SOPs of the even-channels remain unchanged, and the SOPs of the odd-channels are rotated by 90°. Finally, both of them enter the HSPM'. The two polarization components of the even-channels recombine together and reach Port-2 at $(0, -d)$; the two polarization components of the odd-channels also recombine together and reach Port-4 at $(-d, -d)$. For ease of understanding, the SOPs and the relative positions of the light beams after propagation through each component are as shown in the lower part of Fig. 4a.

If an input beam is incident normally on the HSWM' from Port-2 at $(0, -d)$, as shown in Fig. 4b, then the light components of even- and odd-channels reach Port-3 at $(-d, 0)$ and Port-1 at (0, 0), respectively, based on the operating principle in Fig. 4a. The lower part of Fig. 4b depicts the corresponding SOPs and locations. Similarly, Fig. 4c and d show two other cases with inputs at Port-3 and Port-4; the lower parts show the associated SOPs and the positions of the light beams beyond each component. Clearly the routes Port-3→ Port-4 and Port-4→ Port-1 are for even-channels, and those of Port-3→ Port-2 and Port-4→ Port-3 are for odd-channels.

Based on the operating characteristics that are described in Figs. 4 and 5a and b summarize the optical routes for even-channels and odd-channels. In these two figures, the light signal travels clockwise in the order $1 \rightarrow 2 \rightarrow 3 \rightarrow 4 \rightarrow 1$ for even-channels, and travels anti-clockwise in the order $4 \rightarrow 3 \rightarrow 2 \rightarrow 1 \rightarrow 4$ for odd-channels. To avoid he polarization mode dispersion (PMD), no optical path difference may exist between the x- and the y-polarizations along any route. Accordingly, each G and each H must have the same optical thickness. Hence, this optical circulator can serve as a 4-port polarization-independent wavelength-interleaving bidirectional circulator without PMD.

3. Experimental results

The fabricated HSWPs were adopted together with a customer designed LOF to form a 4-port polarization-independent wavelength-interleaving bi-directional circulator at 1550 nm (193.4 THz). The transmission range of the LOF is around 500 nm to 4000 nm [11]. The HSWPs were fabricated using an He–Cd laser of $\lambda = 441.6$ nm and the dichromated gelatin (DCG), as described in our previous work [8]. Their diffraction efficiencies were measured to be $\eta_s = 3\%$ and $\eta_p = 90\%$ with $d = 3.2$ mm. The characteristic parameters of the LOF were measured to be 1.5 dB insertion loss, 100 GHz FSR and 50 GHz channel spacing

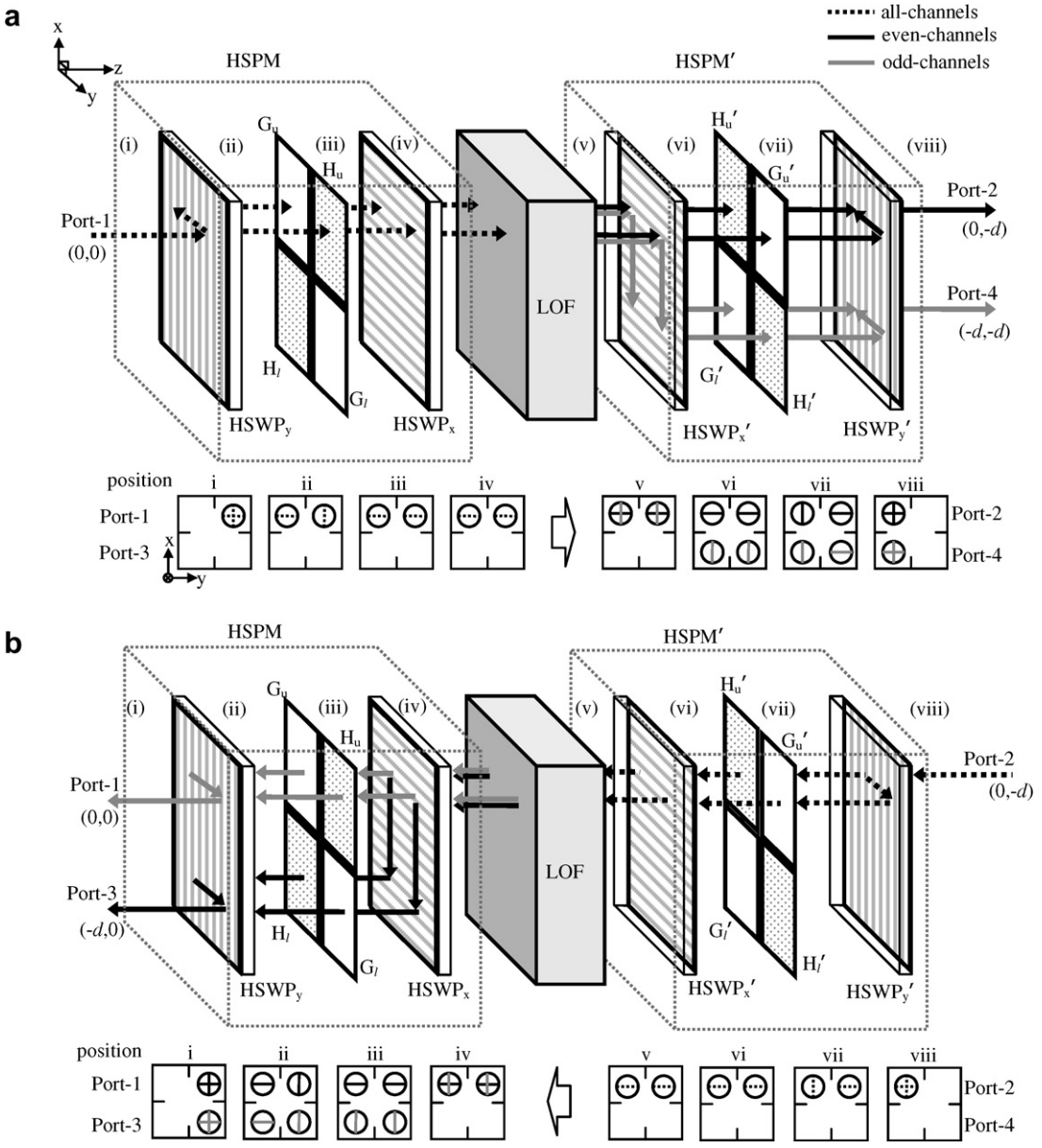

Fig. 4. Structure and operating principles of the 4-port polarization-independent wavelength-interleaving bidirectional circulator as the light signal inputs at (a) Port-1, (b) Port-2, (c) Port-3, and (d) Port-4.

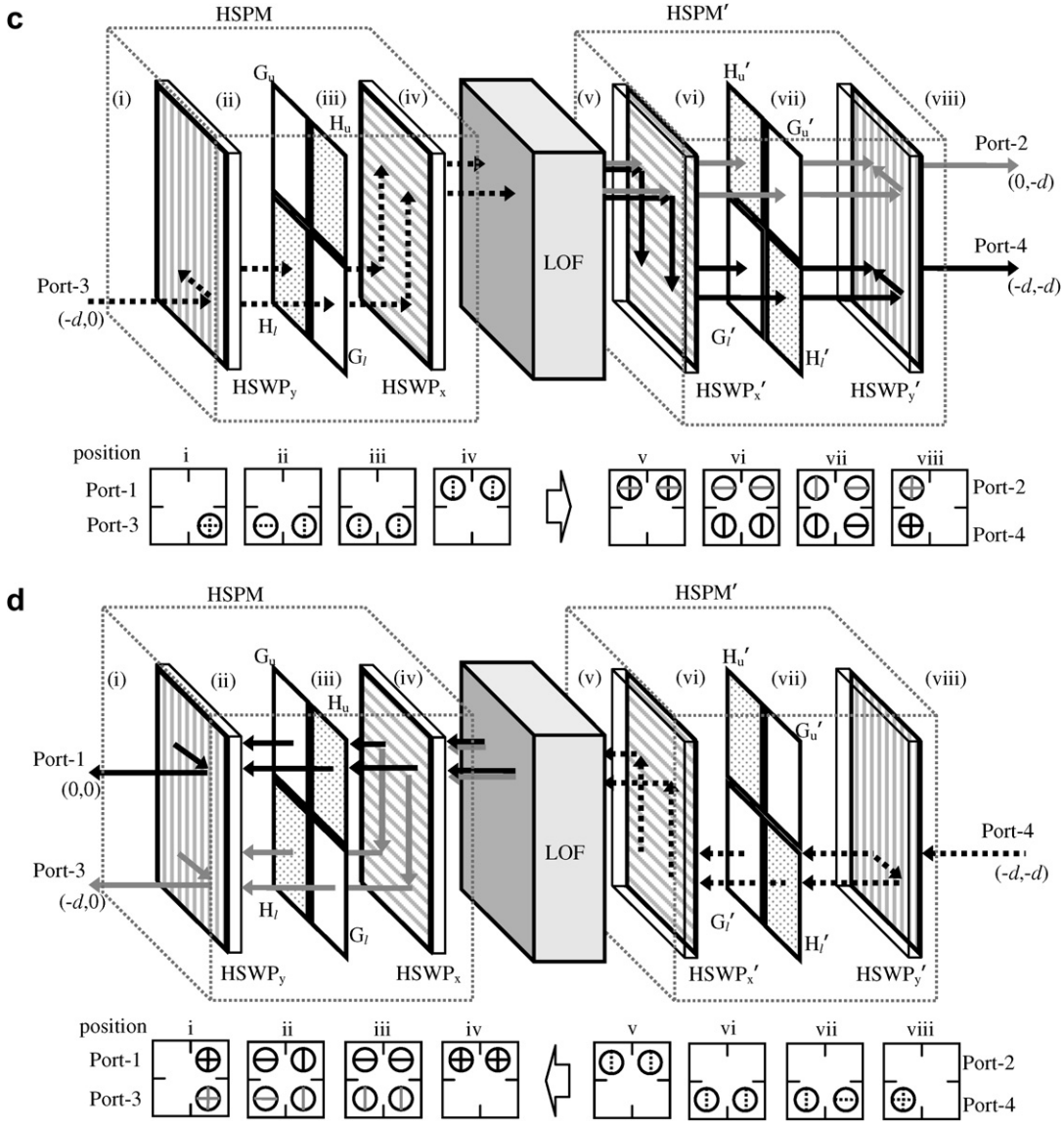

Fig 4. (*continued*)

around 1550 nm. The transmittances of G and H are 0.96 and 0.97, respectively. The characteristic parameters of this prototype device can be estimated from those of each component. Thus, the associated losses and isolation values of this prototype device can be estimated, and are listed in Table 1.

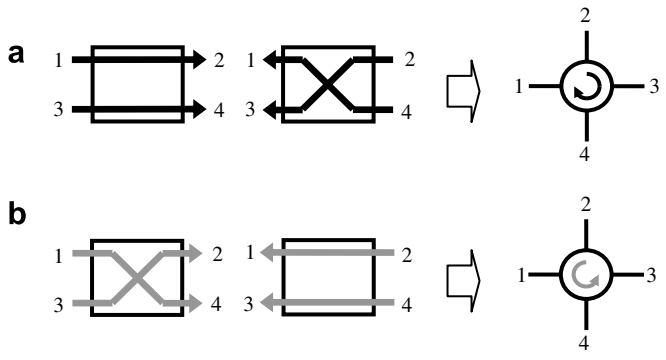

Fig. 5. The equivalent block diagrams for (a) even- and (b) odd-channels.

4. Discussion

Since the fabricated HSWPs have no anti-reflection coatings, a reflection loss of 4% occurs at every boundary. Anti-reflection coatings would reduce the reflection loss to 0.1%. Additionally, if the holographic exposure and the post-processing procedure are controlled more accurately, the HSWPs may exhibit theoretical diffraction efficiencies [12]: $\eta_s < 1\%$ and $\eta_p > 99\%$. These two optimizations significantly enhance the performance of this circulator and the associated parameters are calculated and listed in Table 1b. Fig. 6 plots the theoretical curves of diffraction efficiencies versus wavelengths for the HSWP, based on

Table 1
Associated losses and isolation values (in dB) of the proposed circulator with wavelength 1550 nm and FSR 100 GHz by using (panel a) our fabricated HSWPs and (panel b) ideal HSWPs with anti-reflection coatings and diffraction efficiencies of $\eta_s < 1\%$ and $\eta_p > 99\%$

Even/odd-channel				
Input port	Output port			
	1	2	3	4
Panel a				
1	14.26[a]/14.26[a]	3.20[b]/>24.72	>38.53/>38.53	>29.74/3.50[b]
2	>24.72/3.20[b]	14.26[a]/14.26[a]	3.52[b]/>25.12	>38.53/>38.53
3	>38.53/>38.53	>25.12/3.52[b]	14.26[a]/14.26[a]	3.84[b]/>30.28
4	3.50[b]/>29.74	>38.53/>38.53	>30.28/ 3.843[b]	14.26[a]/14.26[a]
Panel b				
1	>30[a]/>30[a]	<1.83[b]/>41.73	>60.13/>60.13	>41.73/<1.82[b]
2	>41.73/<1.83[b]	>30[a]/>30[a]	<1.82[b]/>41.73	>60.13/>60.13
3	>60.13/>60.13	>41.73/<1.82[b]	>30[a]/>30[a]	<1.83[b]/>41.73
4	<1.82[b]/>41.73	>60.13/>60.13	>41.73/<1.83[b]	>30[a]/>30[a]

All values without a superscript are isolation values.
[a] Return losses.
[b] Insertion losses.

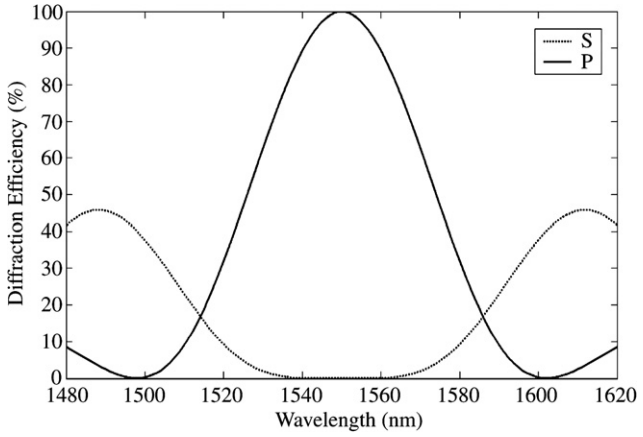

Fig. 6. Calculated diffraction efficiencies of the HSWPs versus wavelength at 1550 nm.

the coupled-wave theory [13]. Clearly, the bandwidth with $\eta_p > 90\%$ and $\eta_s < 1\%$ at a central wavelength of 1550 nm is 16 nm (1542–1558 nm), that is, corresponding to a channel capacity of 41. Under the conditions $\eta_p > 80\%$ and $\eta_s < 1\%$, the channel capacity is increased to 61 and covers almost the entire C-band. The diffraction characteristics of the fabricated HSWP are such that the experimental optical circulator works at a central wavelength of 1550 nm with a bandwidth of 16 nm (41 channels). The fabrication conditions for HSWP [14] can be changed to suit different central wavelengths, and the associated bandwidth increases as the product of the thickness and the index modulation of the recording material is increased [13,14].

5. Conclusion

This study develops an alternative type of 4-port polarization independent wavelength-interleaving bidirectional circulator has been proposed by using an LOF and a pair of orthogonal HSPMs. Each HSPM is composed of two HSWPs, two glass plates and two half-wave plates. The HSWPs were fabricated for a wavelength of 1550 nm and the diffraction efficiencies of the s- and p-polarizations were measured. The characteristic parameters of the LOF were measured. A circulator was thus formed. Its operating principle and performance were discussed. It has such advantages as polarization-independence, compactness, high isolation, and the absence of polarization mode dispersion.

Acknowledgements

This work was partially supported by grants from the National Science Council, Taiwan, ROC, under contract No. NSC-94-2215-E-009-002, and the Lee & MTI Center for Networking at National Chiao Tung University, Taiwan, ROC. The authors would like to thank Dr. J. Chen for providing a Lyot-Ohman filter and information on its associated parameters.

References

[1] J. Hecht, Understanding Fiber Optics, Prentice Hall, NJ, USA, 2002 (Chapter 14).
[2] N. Sugimoto, T. Shintaku, A. Tate, E. Kubota, H. Terui, M. Shimokozono, M. Ishii, Y. Inoue, IEEE Photon. Technol. Lett. 11 (1999) 355.
[3] Y.K. Chen, C.J. Hu, C.C. Lee, K.M. Feng, M.K. Lu, C.H. Chang, Y.K. Tu, S.L. Tzeng, IEEE Photon. Technol. Lett. 12 (2000) 1394.
[4] D.K. Mynbaev, L.L. Scheiner, Fiber-optic Communications Technology, Prentice Hall, NJ, USA, 2001 (Chapter 6).
[5] A.V. Tran, C.J. Chae, R.S. Tucker, IEEE Photon. Technol. Lett. 15 (2003) 975.
[6] Y. Sato, K. Aoyama, IEEE Photon. Technol. Lett. 3 (1991) 1001.
[7] K. Tai, B. Chang, J. Chan, H. Mao, T. Ducellier, J. Xie, L. Mao, J. Wheeldon, IEEE Photon. Technol. Lett. 13 (2001) 320.
[8] J.H. Chen, D.C. Su, J.C. Su, Opt. Express 11 (2003) 2001.

[9] A. Yariv, P. Yeh, Optical Waves in Crystals, J. Wiley and Sons, NY, 1984 (Chapater 5).
[10] S. Cao, J. Chen, J.N. Damask, C.R. Doerr, L. Guiziou, G. Harvey, Y. Hibino, H. Li, S. Suzuki, K.-Y. Wu, P. Xie, J. Lightwave Technol. 22 (2004) 281.
[11] http://www.marketech-crystals.com/.
[12] B.J. Chang, Proc. SPIE. 177 (1979) 71.
[13] H. Kogelnik, Bell Sys. Tech. J. 48 (1969) 2909.
[14] Y.T. Huang, Y.H. Chen, Opt. Lett. 18 (1993) 921.